Title

Resonant electron attachment to N-ethylacetamide: Reduced signature of an intermediate resonant state

Journal

Physical Review A, 114(3)

ISSN

2469-9926

Authors

Chakraborty, Dipayan
Ptasinska, Sylwia
Slaughter, Daniel S

Publication Date

2026-09-01

DOI

10.1103/hpw1-tnzm

Peer reviewed

Resonant electron attachment to N-ethylacetamide: Reduced signature of an intermediate resonant state

Dipayan Chakraborty,[1, 2, *] Sylwia Ptasinska,[1, 3, †] and Daniel S. Slaughter[4, ‡]

[1] *Radiation Laboratory, University of Notre Dame, Notre Dame, IN 46556, USA*
[2] *Present Address: J. Heyrovský Institute of Physical Chemistry, Czech Academy of Sciences, Dolejskova 3, 18223 Prague, Czech Republic*
[3] *Department of Physics & Astronomy, University of Notre Dame, Notre Dame, IN 46556, USA*
[4] *Lawrence Berkeley National Laboratory, Chemical Sciences, Berkeley, California 94720, USA*

(Dated: August 18, 2026)

Dissociative electron attachment to N-ethylacetamide is investigated using velocity map imaging with a tunable electron beam. Previously reported ion-yield spectra reveal two prominent resonant features near 5.5 eV and 8.8 eV across all observed anion channels. Surprisingly, no distinct structure is observed in the intermediate 6–7 eV energy region, where smaller amides typically exhibit an additional resonance associated with amide bond cleavage. For N-ethylacetamide, the absence of a clear feature in this energy region indicates that any corresponding transient negative ion state does not contribute significantly to dissociation. The momentum distributions obtained in the present work reveal distinct dissociation dynamics for different channels. The CH_3^- fragment at 5.5 eV exhibits an anisotropic distribution, indicating a direct dissociation process with finite kinetic energy release. In contrast, the NH^- fragment at 8.8 eV shows an isotropic distribution with near-zero kinetic energy, which suggests a three-body dissociation process. These results demonstrate that the observed resonances correspond to qualitatively different dissociation mechanisms and suggest that the intermediate resonance, if present, does not drive efficient or direct fragmentation in N-ethylacetamide.

PACS numbers: 34.80.Gs, 34.80.Ht

I. INTRODUCTION

Low-energy electron interactions with molecules play a central role in a wide range of physical, chemical, and biological processes, including radiation-induced damage in biomolecules [1–4]. Among these processes, dissociative electron attachment (DEA) is particularly important, as it involves the formation of a transient negative ion (TNI) that can subsequently dissociate into a negative ion and neutral fragments [5, 6]. Such a process is driven by resonant electron capture into temporary anionic states, and the nature, lifetime, and decay pathways of these states govern the fragmentation dynamics [7].

Amide-containing molecules are of particular interest in this context, as the amide bond, which is structurally identical to a peptide bond, is a fundamental structural motif in proteins [8–12]. Understanding electron-induced fragmentation of amides, therefore, provides insight into radiation damage mechanisms at the molecular level. Previous experimental and theoretical studies on small amides, such as formamide and its methylated derivatives, have demonstrated that DEA proceeds through multiple resonant states in the 5–9 eV energy range [8, 11, 12]. In particular, amide bond cleavage is typically associated with distinct resonances near 5 eV and 6–7 eV, while higher-energy features near 9–10 eV contribute to additional fragmentation channels [9, 10].

The resonance energies overlap with the $n_O \rightarrow \pi^*$ and $\pi \rightarrow \pi^*$ excitation manifold of the neutral molecule, suggesting a possible connection to core-excited configurations. However, since available quantum chemical studies address only neutral excitations, and prior experimental and theoretical works do not provide a consensus on the nature of these resonances [8, 10, 13], such assignments should be treated with caution. The formation and stability of these TNI states are strongly influenced by the molecular electronic structure and electron–target interactions. While dipole-bound states may play a role in low-energy electron capture, resonances in the present energy range are more appropriately described in terms of core-excited states arising from electronic excitation and electron correlation effects [10, 13]. The efficiency of such processes depends sensitively on molecular properties such as dipole moment, size, and substitution pattern. Experimental and theoretical studies of methylated amides have shown that increasing molecular size can reduce electron binding energies and alter the character of the accessible anionic states, even when the overall dipole moment remains favorable [14].

Despite this general understanding, the extent to which these resonant features are preserved or modified in more complex amide systems remains an open question. In particular, substitution at the amide nitrogen and carbonyl sites introduces additional electronic and dynamical effects, including changes in orbital energies, increased density of vibrational states, and enhanced coupling between electronic and nuclear degrees

* dipayan.chakraborty@jh-inst.cas.cz
† sptasins@nd.edu
‡ DSSlaughter@lbl.gov

of freedom. These factors can significantly influence the lifetimes and dissociation pathways of TNI states, potentially altering the observable DEA signatures. An important challenge in assigning the m/z = 15 channel arises from the possible contributions of both NH^- and CH_3^-. Dawley and Ptasinska demonstrated this ambiguity in N-methylformamide using partially deuterated molecules [12], whereas our previous study of NEA only tentatively assigned the resonances near 5.5 and 9 eV to CH_3^- and NH^-, respectively, based on analogous fragmentation channels in N-methylformamide [9]. Momentum-resolved measurements therefore provide an opportunity to distinguish these two breakup pathways through their characteristic kinetic-energy and angular distributions.

In this work, we investigate DEA to N-ethylacetamide (NEA), a substituted amide that serves as a model system for examining the influence of molecular environment on electron-driven fragmentation processes. Previous fragment-resolved ion yield measurements by our group have revealed two prominent resonances near 5.5 eV and 9 eV, while no distinct structure is observed in the intermediate 6–7 eV energy region [9]. This absence is notable, as resonances in amide derivatives reported in this energy range are generally associated with efficient fragmentation pathways [8, 11, 12, 15]. The lack of a corresponding feature in NEA therefore raises important questions regarding the nature and fate of the underlying TNI state.

To address the dissociation dynamics associated with the observed resonances, the present study employs velocity map imaging (VMI) to probe the momentum distributions of selected fragment ions. The measurements focus on the CH_3^- channel in the vicinity of 5.5 eV and the NH^- channel near 8.8 eV, enabling a comparative investigation of their kinetic energy release and angular distributions. In contrast to the previous ion-yield measurements, momentum-resolved measurements provide additional information on the dynamics of fragment emission and can reveal resonance-specific features in the kinetic-energy and angular distributions. Such information has previously been shown to be useful for distinguishing contributions from different resonant states in DEA to amide molecules [10]. Here, we use VMI to characterize the dissociation dynamics of the prominent resonances in NEA and to examine whether the momentum distributions provide evidence for any additional resonance-specific contribution across the investigated energy range.

II. EXPERIMENTAL METHOD

Negative ions generated through the DEA process are investigated using the highly differential time-sliced VMI technique. The VMI apparatus, designed and constructed at the Notre Dame Radiation Laboratory, is briefly outlined here. Details of the experimental setup are discussed elsewhere [16, 17]. The experimental arrangement comprises an electron gun, a Faraday cup for measuring the time-averaged electron beam current, a 550 μm diameter needle for generating an effusive molecular beam, and a time-of-flight (TOF)-based VMI spectrometer, housed in an ultrahigh vacuum chamber. The present experiments were conducted under ultra-high vacuum conditions with an approximate base pressure of 10^{-9} mbar. In a crossed-beam configuration, the electron-molecule interaction is between the repeller and extractor electrodes of the VMI spectrometer. A pulsed electron beam, characterized by a width of 200 ns and a repetition rate of 5 kHz, with a time-averaged beam current of $\sim$ 3 nA, crosses the molecular beam at the interaction zone. The molecular beam is generated by evaporating 99.5% pure N-ethylacetamide purchased from Sigma Aldrich through the needle. The interaction results in the production of fragment negative ions through the DEA process. The electron gun, purchased from Kimball Physics, employs a thermally heated tantalum filament with a typical energy spread of 0.8 eV. External to the chamber, a pair of Helmholtz coils is positioned to collimate the low-energy electron beam. After the electron beam pulse, a negative extraction pulse with a 200 ns delay and 150 V amplitude is applied to extract the negative ions from the interaction region into the VMI spectrometer. The extraction delay is optimized for high-quality time-sliced images with minimal scattered electron background. The spectrometer is designed to maintain the VMI condition, such that all ions with a given velocity vector are mapped onto a single point on the detector regardless of their origin. The detector (Photek, USA) comprises two microchannel plates in a chevron configuration, with a phosphor screen positioned behind it. The TOF of the detected ions is determined from the phosphor screen, which generates an AC-coupled pulse upon the passage of an electron cloud. A charge-coupled device camera is employed to capture the time-sliced images.

The molecules in the molecular beam interaction zone are randomly oriented. When low-energy electrons interact with the molecules via the DEA process, the resulting anion fragments are imaged by projecting the quasi-spherical fragment distribution, known as the 'Newton sphere', onto the detector. The kinetic energy distribution and angular distribution of the negative ions are extracted from the image [18]. We apply the velocity slicing technique, where the objective is to capture the central slice of the Newton sphere containing the initial kinetic energy and angular distribution information of the detected ions. We obtain a 50 ns time-sliced image from the central portion of the entire Newton sphere. The typical full-width at half maximum of the Newton sphere is 300 ns. To detect the central slice, we use a gate module to pulse the rear multi-channel plate with an appropriate delay after the extraction pulse. These sliced images depict ions ejected in the plane parallel to the detector containing the electron beam axis. The electron energy calibration was conducted

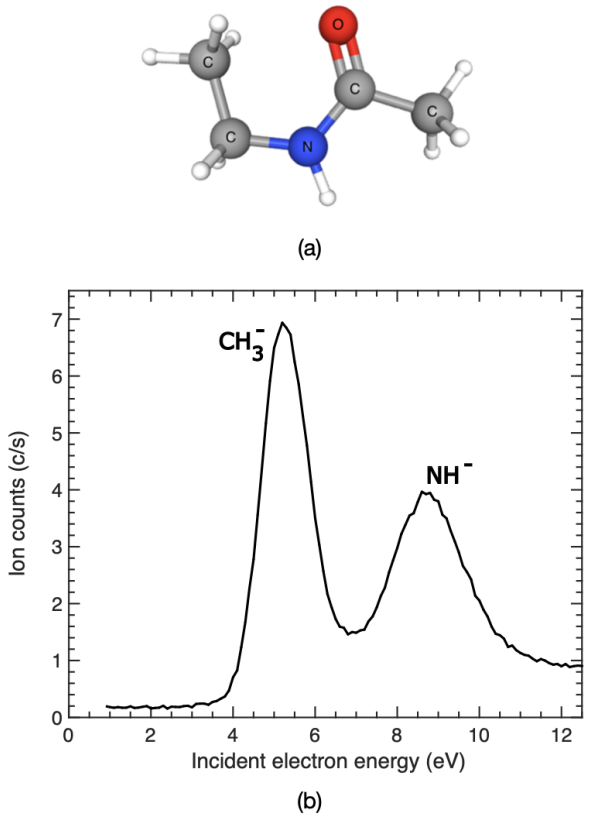

FIG. 1. (a) Molecular structure of the NEA, and (b) Ion-yield curve of m/z 15 ions produced from DEA to NEA in the energy range of 1–13 eV. This figure is adapted from Ref. [9] with permission.

utilizing the resonant peaks of O^- ion yields from DEA to oxygen molecules at 6.5 eV [19]. Kinetic energy distribution measurements were calibrated using the kinetic energy released by O^- ions from O_2 at approximately the same energy. Furthermore, this energy calibration was validated by measuring the kinetic energy of O^- ions produced via DEA to CO_2 at 8.2 eV [20]. The image orientation is calibrated with reference to the well-known asymmetric O^- images resulting from DEA to CO_2 molecules at 8.2 eV [20].

The anion signal pulses detected on the phosphor screen are counted to measure the ion yield curves of the negative ions. Initially, the AC-coupled screen signal undergoes amplification by a fast amplifier and is then routed to a constant fraction discriminator (CFD). The CFD output is linked to the stop input of a nuclear-instrumentation-module standard time-to-amplitude converter (TAC), while the start pulse is generated by a master pulse generator synchronized with the electron-gun pulse. The time difference between the start and stop pulse is the TOF of the negative ions. The TAC output is connected to a multichannel analyzer and a computer for data acquisition. A custom-built LabVIEW-based data acquisition system was employed to acquire the ion yield curves.

III. RESULTS AND DISCUSSION

Dissociative electron attachment to NEA reveals two well-defined resonant features within the investigated energy range, one near 5 eV and another around 9 eV. Fig. 1b exhibits the ion yields of the dominant fragment channels at $m/z = 15$. We tentatively assign the lower and higher energy resonances to the two-body dissociation producing CH_3^- and three-body producing NH^-, respectively, following the prior analysis [12] of the analogous dissociation channels of N-methylformamide. A comprehensive picture emerges when considering the full set of fragment ion yields reported previously for NEA [9]. In addition to the dominant m/z 15 channels, multiple dissociation pathways—including those leading to CH_3CO^-, $CH_3CH_2NH^-$, and CH_3CONH^- have been systematically investigated [9]. Across all observed channels, the DEA spectra consistently exhibit only two resonant features, centered near 5–5.5 eV and ∼9 eV, with no evidence of an intermediate structure near 6–7 eV. This absence is consistent across the different fragment ions, indicating that the lack of a resonance in this energy range is not channel-specific but reflects the overall electronic structure and dissociative behavior of the system.

A broader perspective from smaller amides established that the energy-dependent resonance structures in NEA contrast with other amides [8, 9, 11, 12, 15]. Previous DEA studies on prototypical amides such as formamide, N-methylformamide, N-ethylformamide, and N,N-dimethylformamide show that amide bond dissociation is typically mediated by multiple resonant states in the 5–8 eV energy range, often resulting in structured ion-yield curves with distinct features near 5 eV and 6–7 eV [8, 11]. In addition, these systems frequently exhibit higher-energy resonances near 9–10 eV that contribute to other fragmentation pathways [10]. Such complex multi-resonance behavior is a recurring characteristic of DEA in amide-containing molecules. This behavior is not restricted to formamide derivatives only. DEA studies of acetamide have reported a distinct resonance near 6.2 eV in the OCN^- production channel, indicating that intermediate-energy TNI states can contribute to fragmentation in acetamide derivatives [15]. Interestingly, fragment-resolved measurements by Muftakov *et al.* did not reveal a similarly pronounced feature in the NH_2^- channel, although a weak shoulder in the 6–7 eV region may be observed upon close inspection [21]. These observations suggest that the contribution of the intermediate resonance can be strongly channel dependent. In contrast, no comparable structure is observed in any of the measured NEA fragmentation channels. The formation and stability of TNI states are known to be sensitive to molecular size and substitution. For example,

studies of methylated amides have shown that electron binding energies can vary systematically with substitution, reflecting changes in molecular size and electronic structure [14]. While these studies concern low-energy dipole-bound states, they highlight the broader sensitivity of electron attachment processes to molecular modification.

Within this established understanding, the absence of any intermediate resonance near 6–7 eV in NEA is puzzling. The molecule exhibits a low-energy resonance near 5–5.5 eV and a higher-energy feature near 9 eV, which are generally interpreted in terms of different classes of temporary anion states. However, the detailed electronic character of these resonances remains under debate. Previous studies have proposed that electron attachment in this energy range proceeds via core-excited resonances, including dipole-supported configurations [8], while alternative interpretations invoke more conventional doubly excited Rydberg-type Feshbach resonances [13].

Consistent with this, recent experimental and theoretical investigations have revealed multiple, overlapping resonances in the 5–7 eV region and highlighted the difficulty of assigning a unique electronic character to these states [10]. Against this backdrop, the absence of a corresponding feature in the 6–7 eV region in NEA suggests that such a resonance is not a universal property of the amide functional group. This observation forms the central question of the present study: why does NEA lack the intermediate resonance near 6–7 eV that is observed in other small amides?

A. The 5.5 eV resonance

For NEA, the low-energy resonance is observed near 5.5 eV in the m/z 15 channel, corresponding predominantly to the formation of CH_3^- fragments. Fig. 2a shows the time-slice image of DEA to NEA at 5.5 eV electron energy. The electron beam direction is from bottom to top through the center of the image. The image is dominated by a pronounced ring, which corresponds to CH_3^- ions produced via the 5.5 eV resonance with well-defined kinetic energy release. The presence of a single ring suggests that one resonant state may initiate the dissociation dynamics at this energy.

The appearance of this resonance is consistent with the electronic structure of amide systems. The lowest unoccupied orbital in simple amides is the π^* (C=O) orbital localized on the carbonyl group, and electron attachment into this orbital can give rise to a valence π^* shape resonance. However, such shape resonances are typically short-lived and are unlikely to directly lead to bond cleavage. Indeed, both experimental and theoretical studies have shown that, in amide systems, valence π^* shape resonances lie at lower energies and do not efficiently drive DEA in the 5–7 eV range [8]. Instead, fragmentation in this energy region is generally attributed

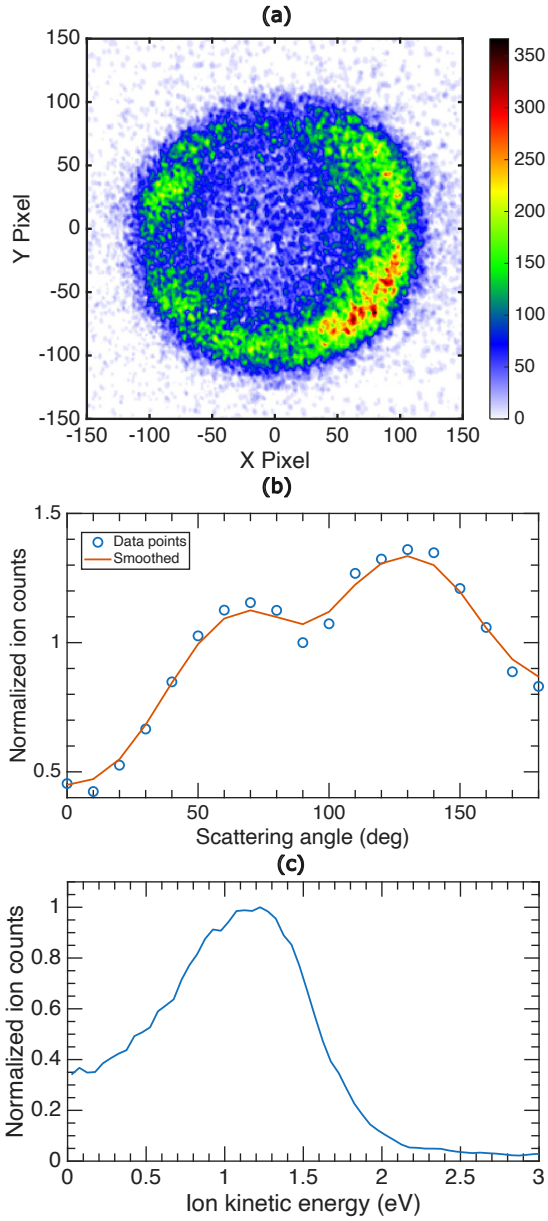

FIG. 2. (a) Time-slice image of CH_3^- ions from DEA to NEA at 5.5 eV resonance. The electron-beam direction is from bottom to top through the center of the image. (b) Angular distribution of the CH_3^- ions at the same electron energy with respect to the electron beam direction. (c) Kinetic energy distributions of the CH_3^- ions at the same electron energy. The distribution shown is obtained after integration over the entire 2π angle about the direction of the electron beam and normalized to the peak value.

to longer-lived core-excited resonances, including dipole-supported configurations, or to coupling between valence and dissociative states.

In particular, momentum-resolved studies and theoretical analyses of formamide have identified resonances in the 5–7 eV region as electronic Feshbach resonances involving excitation of the neutral core and electron cap-

ture into diffuse orbitals, which can provide sufficient lifetime for dissociation [10, 13]. In this context, the observed 5.5 eV resonance in NEA may involve similar core-excited character or state mixing, rather than direct dissociation from a simple π^* shape resonance.

The kinetic energy (KE) distributions of the CH_3^- ions further support this interpretation. The kinetic energy of the fragment ions is extracted from the time-sliced image as described previously [7, 16]. The KE spectra show a peak near 1.2 eV, indicating that a significant fraction of the available excess energy is released into fragment translation energy. Such a relatively narrow kinetic energy distribution and the pronounced ring structure in the momentum image suggest that the dissociation proceeds via a direct, non-statistical pathway, where fragmentation occurs on a repulsive potential energy surface without extensive intramolecular energy redistribution. Importantly, this dynamical behavior does not uniquely determine the nature of the underlying resonant state. Even in cases where electron attachment proceeds via core-excited or mixed electronic configurations, coupling to a specific dissociative coordinate can still result in prompt fragmentation with well-defined kinetic energy release.

The formation of CH_3^- ions may proceed through two fragmentation pathways previously identified for NEA [9]. Two energetically accessible channels are

$$\begin{aligned} CH_3CO(NH)CH_2CH_3 + e^- &\rightarrow (CH_3CO(NH)CH_2CH_3)^{*-} \\ &\rightarrow \begin{cases} CH_3^- + CONHCH_2CH_3 & (a) \\ CH_3^- + CH_3CO(NH)CH_2 & (b) \end{cases} \end{aligned}$$

Channel (a) corresponds to cleavage of the C–C bond adjacent to the carbonyl group (threshold energy of 3.61 eV), whereas channel (b) involves fragmentation within the ethyl substituent (threshold energy of 3.43 eV) [9]. While electron attachment into the π^* (C=O) orbital is expected to initially localize excess charge near the carbonyl site, thereby promoting bond weakening in its vicinity, the dissociation dynamics are not necessarily restricted to this region. In a molecule of the size of NEA, efficient intramolecular vibrational energy redistribution can occur prior to fragmentation, enabling cleavage at remote sites. Consequently, although channel (a) is electronically intuitive, the slightly lower threshold of channel (b) makes it energetically competitive, and both pathways may contribute to the observed CH_3^- signal.

Despite the presence of multiple energetically accessible dissociation pathways, the VMI image exhibits a single dominant ring structure with a slight forward–backward asymmetry (Fig. 2a). In addition, enhanced intensity is observed along two preferential directions, approximately near 60° and 135°, indicating anisotropic fragment emission. Correspondingly, the angular distribution (Fig. 2b) exhibits local minima near 0°, 90°, and 180°. Such anisotropy suggests that the dissociation retains a memory of the electron attachment step and that electron capture is not equally probable for all molecular orientations. In DEA, the fragment angular distribution is governed primarily by the orientation dependence of electron attachment to the TNI and can therefore provide information on the character of the underlying resonant state. Similar use of angular distributions to probe resonance character has been demonstrated in momentum-imaging studies of DEA to formamide [10]. Although the low symmetry of NEA precludes a rigorous symmetry assignment of the resonance, the presence of multiple maxima and minima suggests that the attachment process likely involves contributions from one or more resonances that dissociate promptly, resulting in a non-uniform angular distribution [22]. Since both CH_3^- formation pathways are expected to originate from the same underlying TNI state, they should exhibit similar angular distributions. Consequently, the observed image most likely represents a superposition of contributions from both fragmentation channels.

These observations suggest that the 5.5 eV feature in NEA arises from a TNI state with significant valence character, likely involving mixed or core-excited configurations rather than a simple π^* shape resonance. This state leads to CH_3^- formation via cleavage in both the acetyl and ethyl moieties, reflecting the interplay between initial electron attachment and subsequent dissociation dynamics.

B. Origin of the missing intermediate resonance in NEA

The absence of the intermediate resonance near 6–7 eV in NEA, despite its well-established presence in formamide derivatives, indicates a fundamental change in the underlying electron attachment dynamics. As discussed in the previous sections, DEA to amide-containing molecules typically proceeds through multiple resonant states in the 5–9 eV energy range, arising from both valence and core-excited Rydberg configurations [8, 10, 11]. Electronic structure calculations and recent experimental studies indicate that, in this energy range, the observed resonances could be electronic Feshbach resonances arising from electronic excitation and electron correlation effects [10, 13]. The absence of such a feature in the 6–7 eV region therefore suggests that no well-separated intermediate resonant state is present or contributes significantly to the DEA dynamics in this system.

A key factor governing the formation of such resonances is the ability of the molecule to temporarily capture the incident electron. In many amides, this process can involve dipole-supported precursor states that facilitate electron capture into more localized valence or core-excited configurations [8]. The efficiency of this

process depends sensitively on electronic correlation, the molecular dipole moment and the electronic structure of the molecule. In this context, methyl substitution can modify the charge distribution and available electronic configurations, thereby influencing the formation and stability of TNI states and their coupling to dissociative channels.

In NEA, substitution at both the nitrogen and carbonyl-adjacent positions introduces a more extended and asymmetric alkyl environment compared to formamides. This modification can influence the intermediate resonance through several mechanisms. First, substitution can alter the electronic structure of the molecule, modifying the energies and character of the TNI states and their coupling to dissociative channels. Second, the larger molecular framework provides a higher density of vibrational states, which may facilitate energy redistribution following electron attachment. Under such conditions, the lifetime of a potential intermediate TNI may be reduced, making it less likely to compete with autodetachment and thereby suppressing observable dissociation [23, 24].

An additional contributing factor is the reduced molecular symmetry of NEA. While the amide functional group itself is approximately planar and can be described by local C_s symmetry, the entire NEA molecule belongs to the C_1 point group due to asymmetric alkyl substitution. In contrast, smaller amides often retain approximate planar symmetry that allows clearer separation of electronic states into distinct symmetry classes (e.g., A′ and A″). The loss of such symmetry constraints in NEA facilitates mixing between electronic states of different character, including valence and core-excited configurations. This increased state mixing can lead to broadening and destabilization of the intermediate resonance, effectively reducing its lifetime and causing it to merge with the continuum [22].

Additionally, the formation of electronic Feshbach resonances in the 6–7 eV region requires sufficient coupling between the relevant continuum electronic state(s) and nuclear dynamics that may allow resonances in the continuum to become electronically bound. In smaller amides, these resonances manifest as distinct features contributing to amide bond cleavage [10, 25]. However, if the electronic structure is perturbed such that the corresponding excited state becomes strongly mixed with the continuum, the resonance may lose its identity and effectively collapse [22, 24]. In this scenario, electron attachment in the intermediate energy range would predominantly lead to prompt autodetachment rather than fragmentation, resulting in the absence of any detectable feature in the ion-yield spectrum.

It is also important to note that the absence of the intermediate resonance in NEA is observed consistently across all fragmentation channels [9]. This rules out the possibility that the corresponding state is merely redistributed among competing dissociation pathways. Instead, it suggests that the underlying TNI state is either not formed or is too short-lived to produce measurable DEA signals. In contrast, the lower energy resonance near 5 eV and the higher energy resonance near 8.8 eV remain clearly observable, indicating that these states are comparatively robust against substitution and retain sufficient lifetime to drive dissociation.

Taken together, these observations suggest that any intermediate resonance in the 6–7 eV region is highly sensitive to the local electronic environment of the amide bond. While the low- and high-energy resonances appear to be general features of DEA in amide systems, the presence of an additional intermediate feature is not intrinsic to the amide functional group itself. Rather, such a feature likely arises from closely spaced TNI states whose accessibility depends on the details of the molecular electronic structure, electron correlation, and nuclear dynamics, all of which can be significantly modified by molecular substitution. The absence of this intermediate resonance in NEA therefore indicates that substituent effects can strongly influence the structure and accessibility of TNI states in amide-containing molecules.

C. The 8.8 eV resonance

Fig. 3a shows the time-sliced image of NH^- from DEA to NEA at 8.8 eV. The image corresponds to a 50 ns time-sliced measurement, providing a two-dimensional projection of the three-dimensional momentum distribution of the fragment ions. The electron beam direction is from bottom to top through the center of the image, which serves as the reference axis for evaluating angular anisotropy.

A dominant feature of the image is the intense, localized central spot, indicating that the majority of NH^- ions are formed with near-zero kinetic energy (see Fig. 3b). The absence of any pronounced higher kinetic energy structure confirms that the kinetic energy release in this channel is minimal. The angular distribution of the NH^- ions is essentially isotropic, as evidenced by the intensity distribution. Such isotropy suggests that the fragmentation does not retain a strong memory of the initial electron attachment direction. This may arise from three-body dissociation dynamics or from the contribution of multiple fragmentation pathways and geometries, leading to an overall averaging of the angular distribution. In addition to the central feature, weak intensity at larger radii is observed, corresponding to ions with slightly higher kinetic energies (peaking near 1.5–2 eV). These counts are likely attributable to contributions from CH_3^- ions. Given the finite energy resolution in the present measurements and the broad nature of the resonances, some overlap of contributions from the 5.5 eV resonance is expected; however, a contribution from residual background O^- ions cannot be completely excluded, and therefore the observed higher-kinetic-energy component may contain contributions from both CH_3^-

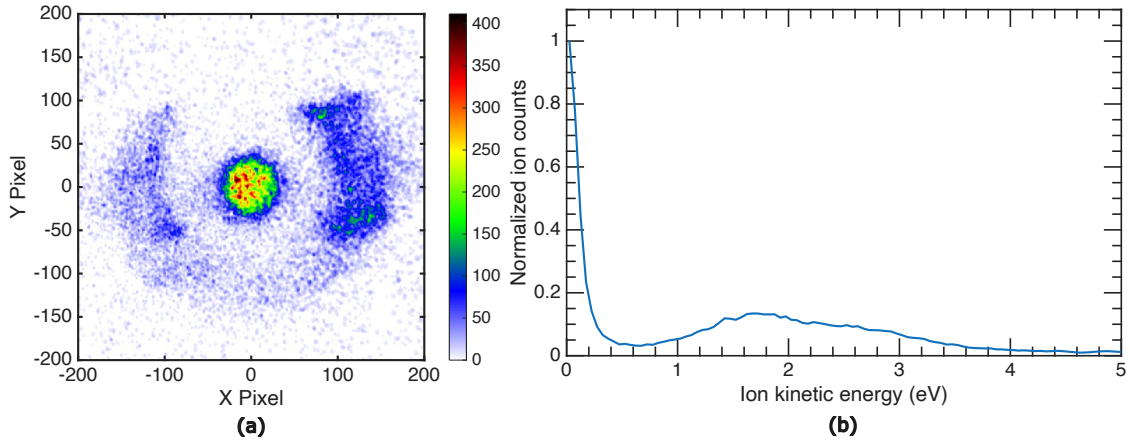

FIG. 3. (a) Time-slice image of NH^- ions from DEA to NEA at 8.8 eV resonance. The electron-beam direction is from bottom to top through the center of the image. An isotropic distribution is observed. (b) Kinetic energy distributions of the NH^- ions at the same electron energy. The intense near-zero eV peak corresponds to the formation of NH^- ions, whereas the broader higher kinetic energy component may arise from contributions of CH_3^- ions, as described in the text.

and background O^-.

The energetics of this channel further support this interpretation. The threshold energy for NH^- formation in NEA is approximately 7 eV [9], and the observed near-zero kinetic energy distribution suggests that only a small fraction of the excess energy is converted into translational motion. Instead, the dissociation proceeds through a statistical decay mechanism, where the TNI undergoes significant intramolecular vibrational energy redistribution prior to fragmentation. Similar isotropic and low kinetic energy behavior has been reported for three-body fragmentation channels in other amide systems [10].

Overall, the VMI results indicate that NH^- formation at the 8.8 eV resonance proceeds via a low-energy, three-body dissociation pathway with isotropic angular distribution that is dominated by statistical decay. The absence of any anisotropic features or structured kinetic energy release suggests that fragmentation is not driven by a direct dissociation pathway, but rather by highly mixed TNI states. This behavior is consistent with a scenario in which electronic excitation at higher energies leads to strong coupling between electronic and nuclear degrees of freedom, resulting in efficient energy redistribution prior to bond cleavage.

IV. CONCLUSION

In this work, we have investigated DEA to NEA using VMI measurements of the dominant anion channels, supported by previously reported fragment-resolved ion yield measurements [9]. The combined analysis identifies two prominent resonant features near 5.5 eV and 8.8 eV, each of which is associated with multiple fragmentation channels. Notably, no clear or well-resolved structure is detected in the intermediate 6–7 eV energy region.

The VMI measurements provide insight into the dissociation dynamics of two different fragment channels. The CH_3^- channel exhibits a pronounced anisotropic angular distribution with a well-defined ring structure, indicating direct dissociation following electron attachment via a transient negative ion state. This observation highlights the coexistence of distinct dynamical pathways originating from the same underlying resonant state for the 5.5 eV feature. In contrast, the NH^- channel shows a predominantly isotropic and low kinetic energy distribution, suggesting a less direct, three-body dissociation, possibly involving energy redistribution prior to fragmentation.

Within the broader context of DEA to amide-containing molecules, previous studies have shown that multiple resonant states can contribute in the 5–8 eV energy range, reflecting closely spaced valence and core-excited configurations. The absence of a distinct intermediate feature in the previously measured ion yields of NEA, together with the absence of an additional resonance-specific signature in the present $m/z = 15$ momentum distributions, provides no evidence for an intermediate resonance contributing to the observed DEA channels. This behavior can be understood in terms of substituent-induced modifications to the electronic structure, including reduced symmetry, enhanced state mixing, and increased coupling to autodetachment, all of which can suppress or broaden the contribution of weakly bound TNI states.

Importantly, the present results do not exclude the existence of an intermediate resonant state in NEA. Rather, they indicate that if such a state is present, it is likely short-lived, or too weak to produce a measurable signature in the DEA observables under the current experimental conditions. This emphasizes that not all electronically accessible states necessarily manifest as distinct features in fragment yields or momentum distributions.

Overall, the results demonstrate that while the low-

and high-energy resonances are robust features of DEA in amide systems, the presence of an intermediate feature is highly sensitive to molecular substitution and local electronic structure. These findings provide new insight into how electronic structure and nuclear dynamics jointly govern the formation and decay of TNI states in complex molecules. Further studies combining improved electron-energy resolution, together with advanced theoretical treatments, would be valuable for clarifying the role and detectability of such weak or short-lived resonances.

V. ACKNOWLEDGEMENTS

DC acknowledges the Grant agency of the Czech Republic (Grant number 25-16240L) and the FWF Austrian Science Fund (Grant number 10.55776/PIN4290924). DC and SP acknowledge the U.S. Department of Energy Office of Science, Office of Basic Energy Sciences under Award Number DE-FC02-04ER15533 (NDRL No: 5504). Work at Lawrence Berkeley National Laboratory was supported by the U.S. Department of Energy, Office of Science, Office of Basic Energy Sciences, Division of Chemical Sciences, Biosciences and Geosciences under Contract Number DE-AC02-05CH11231.

[1] J. D. Gorfinkiel and S. Ptasinska, Journal of Physics B: Atomic, Molecular and Optical Physics **50**, 182001 (2017).
[2] S. Ptasinska, M. T. d. N. Varella, M. A. Khakoo, D. S. Slaughter, and S. Denifl, The European Physical Journal D **76**, 179 (2022).
[3] I. I. Fabrikant, S. Eden, N. J. Mason, and J. Fedor (Academic Press, 2017) pp. 545–657.
[4] B. Boudaïffa, P. Cloutier, D. Hunting, M. A. Huels, and L. Sanche, Science **287**, 1658 (2000).
[5] G. J. Schulz, Rev. Mod. Phys. **45**, 423 (1973).
[6] E. Illenberger and J. Momigny, *Gaseous Molecular Ions: An Introduction to Elementary Processes Induced by Ionization*, Topics in Physical Chemistry (Steinkopff, 2013).
[7] A. Paul, D. S. Slaughter, S. Ptasinska, D. Nandi, I. Carmichael, J. D. Gorfinkiel, and D. Chakraborty, Phys. Rev. A **111**, 042804 (2025).
[8] Z. Li, M. Ryszka, M. M. Dawley, I. Carmichael, K. B. Bravaya, and S. Ptasińska, Phys. Rev. Lett. **122**, 073002 (2019).
[9] D. Chakraborty, L. Eckermann, I. Carmichael, and S. Ptasińska, J Chem. Phys. **153**, 224306 (2020).
[10] G. Panelli, A. Moradmand, B. Griffin, K. Swanson, T. Weber, T. N. Rescigno, C. W. McCurdy, D. S. Slaughter, and J. B. Williams, Phys. Rev. Res. **3**, 013082 (2021).
[11] T. Hamann, A. Edtbauer, F. Ferreira da Silva, S. Denifl, P. Scheier, and P. Swiderek, Phys. Chem. Chem. Phys. **13**, 12305 (2011).
[12] M. M. Dawley and S. Ptasińska, Int. J. Mass Spectrom. **365-366**, 143 (2014), special issue: Tilmann Märk.
[13] J. Fedor, Phys. Rev. Lett. **124**, 199301 (2020).
[14] C. Desfrançois, V. Périquet, S. Carles, J. P. Schermann, D. M. A. Smith, and L. Adamowicz, J Chem. Phys. **110**, 4309 (1999).
[15] C. Koenig-Lehmann, J. Kopyra, I. Dabkowska, J. Kocisek, and E. Illenberger, Phys. Chem. Chem. Phys. **10**, 6954 (2008).
[16] D. Chakraborty, D. S. Slaughter, and S. Ptasinska, Phys. Rev. A **108**, 052806 (2023).
[17] D. Chakraborty, G. Kharchilava, I. Carmichael, and S. Ptasinska, J. Phys. B: At. Mol. Opt. Phys. **56**, 245202 (2024).
[18] P. Nag, M. Polášek, and J. Fedor, Phys. Rev. A **99**, 052705 (2019).
[19] D. Rapp and D. D. Briglia, J. Chem. Phys. **43**, 1480 (1965).
[20] D. S. Slaughter, H. Adaniya, T. N. Rescigno, D. J. Haxton, A. E. Orel, C. W. McCurdy, and A. Belkacem, J. Phys. B: At. Mol. Opt. Phys. **44**, 205203 (2011).
[21] M. V. Muftakhov, R. F. Tuktarov, and V. A. Mazunov, Chem. Phys. Reports. **18(3)**, 413 (1999).
[22] W. Domcke, Physics Reports **208**, 97 (1991).
[23] J. Simons, The Journal of Physical Chemistry A **112**, 6401 (2008), pMID: 18630888.
[24] H. Hotop, M.-W. Ruf, M. Allan, and I. Fabrikant (Academic Press, 2003) pp. 85–216.
[25] T. P. M. Goumans, F. A. Gianturco, F. Sebastianelli, I. Baccarelli, and J. L. Rivail, Journal of Chemical Theory and Computation **5**, 217 (2009), pMID: 26609835.